

## Article

# Evaluation of Thermal Stability of DNA Oligonucleotide Structures Embedded in Hydrogels

Daisuke Yamaguchi, Masatoshi Yoshida and Shu-ichi Nakano \* 

Department of Nanobiochemistry, Faculty of Frontiers of Innovative Research in Science and Technology (FIRST), Konan University, 7-1-20, Minatojima-Minamimachi, Chuo-ku, Kobe 650-0047, Japan

\* Correspondence: shuichi@konan-u.ac.jp

**Abstract:** Understanding the self-assembly and hybridization properties of DNA oligonucleotides in confined spaces can help to improve their applications in biotechnology and nanotechnology. This study investigates the effects of spatial confinement in the pores of hydrogels on the thermal stability of DNA oligonucleotide structures. The preparation of oligonucleotides embedded in agarose gels was simple, whereas the preparation of oligonucleotides embedded in polyacrylamide gels was required to remove unpolymerized monomers. In the latter case, a method for rehydrating a washed dry gel with a buffer solution containing oligonucleotides was developed. Fluorescence measurements of oligonucleotides bearing fluorescent probes revealed no significant influence of the internal environment of the gel pores on the stability of DNA duplex, hairpin, and G-quadruplex structures. Moreover, the effects of poly(ethylene glycol) on the stability of DNA structures in the gels were similar to those in solutions. It is likely that the oligonucleotides are not strongly constrained in the gels and may be preferentially located in a water-rich environment in the gel matrix. The gel preparation was also applied to the assessment of the stability of DNA structures under the conditions of a reduced number of water molecules. The studies using hydrogels provide insights into the ability of self-assembly and hybridization of oligonucleotides in confined environments and under low-water-content conditions.

**Keywords:** oligonucleotide; hairpin; G-quadruplex; melting temperature; agarose gel; polyacrylamide gel; poly(ethylene glycol); confinement



**Citation:** Yamaguchi, D.; Yoshida, M.; Nakano, S.-i. Evaluation of Thermal Stability of DNA Oligonucleotide Structures Embedded in Hydrogels. *DNA* **2022**, *2*, 302–313. <https://doi.org/10.3390/dna2040021>

Academic Editor: Paul Chastain

Received: 19 October 2022

Accepted: 28 November 2022

Published: 14 December 2022

**Publisher's Note:** MDPI stays neutral with regard to jurisdictional claims in published maps and institutional affiliations.



**Copyright:** © 2022 by the authors. Licensee MDPI, Basel, Switzerland. This article is an open access article distributed under the terms and conditions of the Creative Commons Attribution (CC BY) license (<https://creativecommons.org/licenses/by/4.0/>).

## 1. Introduction

Synthetic nucleic acids are promising molecules in the fields of biotechnology and nanotechnology. The self-assembly and hybridization of oligonucleotides can be predicted and controlled using the thermodynamic data of Watson–Crick base pairing obtained using simple aqueous solutions [1]. However, oligonucleotides for technological applications are frequently required to function in sterically crowded and spatially confined conditions, such as in living cells and at the interface of solid materials [2,3]. These conditions may change the thermodynamic and kinetic behaviors of nucleic acid interactions. Many studies have demonstrated that the molecular environments inside a living cell and on a material interface have a significant influence on the efficiency of DNA hybridization, RNA structural stability, and gene expression [4–7]. In vitro experiments using mixed solutions of water and water-soluble neutral polymers, such as poly(ethylene glycol) (PEG) and polysaccharides, enable a quantitative and reproducible analysis of the effects of molecular environments. The studies have elucidated the contribution of molecular crowding that produces excluded volume effects and changes solvent properties to the structures, interactions, and functions of polynucleotides and oligonucleotides [8]. In addition to molecular crowding, spatial confinement in small spaces that produces boundary effects is significant in cells: the crosslinked actin filament network is assembled in the cytoplasm, and the intracellular gelation of nucleic acids, proteins, and peptides results in hydrogel formation

and phase separation [9]. The confined environment in cell nuclei facilitates the assembly and compaction of DNA as part of bacterial genome organization and chromosome localization [10–13]. Furthermore, studies using crosslinking polymers have demonstrated that the formation of intracellular crosslinked networks increases T-cell expansion and decreases DNA replication and protein synthesis [14,15]. Considering the effects of confinement is also important for developing biosensing devices and drug delivery systems, where molecules are entrapped in small spaces such as pores, cavities, chambers, nanochannels, or droplets [16].

Hydrogels with a porous network structure have emerged as potential candidates for biomedical applications such as drug delivery carriers and biomimetic scaffolds [17,18]. The gel matrix, whose pore size is tunable by preparation conditions, can permeabilize small molecules and control the release of embedded molecules, making it useful as a scaffold for tissue engineering. The embedded molecules are confined and have reduced conformational space and translational motion. Changes also occur in the solvent properties of water, such as viscosity, molecular activity, and dielectric constant [19–21]. Accordingly, the internal environment of gel pores has a significant impact on the static and dynamic properties of embedded molecules. Studies have demonstrated the stabilization of several protein structures in agarose and polyacrylamide gels, which is consistent with the model of elimination of expanded unfolded conformations in confined spaces [2,22,23]. The stability of protein structures is also influenced by attractive and repulsive interactions with the walls of gel pores and by changes in the solvent properties of water in the immediate environment of gel filaments [24,25]. In contrast to proteins, the effects of the confined environment on nucleic acids have not been thoroughly studied despite several computer simulation studies showing an increase in the efficiency of RNA folding [26,27], changes in the denaturation profile of a DNA duplex [28–30], and an increase in the rigidity of a DNA G-quadruplex [31]. There are also several experimental studies that have shown that the confinement of DNA and RNA molecules to small reaction volumes of vesicles, two-phase aqueous systems, nanocages, and gels affects DNA structural stability, assembly, and ribozyme catalytic activity [32–38]. It is important to note that the magnitude of confinement effects varies depending on the nucleotide length and the pore size of the gel. Agarose and polyacrylamide gels are the most commonly used media for nucleic acid electrophoresis, such as for separating different fragment lengths and analyzing their structures and interactions by gel shift and temperature gradient gel electrophoresis assays. In this study, we investigate the preparation of the gels for assessing the effects of confinement on the stability of the DNA duplex (DS), hairpin (HP), and G-quadruplex (GQ) structures used in biotechnology and nanotechnology applications. In our previous study, UV spectroscopy was used to analyze the effects of confinement in agarose and polyacrylamide gel pores on polynucleotides and oligonucleotides [39]. However, due to the high UV absorption of the gels, the UV spectroscopic study had limitations, yielding ambiguous results about the effects of confined spaces on the base-pair stability of DNA oligonucleotides. Here, we develop new platforms for investigating the stability of oligonucleotide structures noncovalently embedded in gels. We also prepared low-water-content gels for assessing the stability of DNA structures under the conditions of a reduced number of water molecules. The findings provide a basis for predicting and controlling the self-assembly and hybridization of oligonucleotides in confined environments and under low-water-content conditions.

## 2. Materials and Methods

### 2.1. Preparation of Buffer Solutions and Oligonucleotides

All reagents used to prepare buffer solutions were purchased from Wako Chemicals (Osaka, Japan), except the disodium salt of ethylenediamine-*N,N,N',N'*-tetraacetic acid (EDTA), which was purchased from Dojindo (Mashiki, Kumamoto, Japan). The buffer solutions consisted of 1 M NaCl, 10 mM Na<sub>2</sub>HPO<sub>4</sub>, and 1 mM Na<sub>2</sub>EDTA, adjusted to pH 7.0. PEG-containing solutions were adjusted to pH 7.0 after dissolving PEG in the buffer solution.

DNA oligonucleotides labeled with 6-carboxyfluorescein (FAM) at the 5'-end and/or 4-((4-(dimethylamino)phenyl)azo)benzoic acid (Dabcyl) or 6-carboxytetramethylrhodamine (TAMRA) at the 3'-end were either synthesized using an ABI 3400 DNA synthesizer (Applied Biosystems: Waltham, MA, USA), followed by purification by polyacrylamide gel electrophoresis or purchased as high-performance liquid chromatography-grade from Hokkaido System Science (Sapporo, Hokkaido, Japan) and Fasmac (Atsugi, Kanagawa, Japan). Oligonucleotide concentrations were determined from the absorbance at 260 nm measured with a UV-1800 spectrophotometer (Shimadzu: Kyoto, Japan), using molar extinction coefficients of nucleotides and conjugated dyes at 260 nm.

### 2.2. Preparation of Agarose Gels and Measurement of Their Phase Transition Temperatures

The agarose gel used in this study had a relatively high gelling temperature (Agarose LE; Wako Chemicals). The agarose powder was added to the buffer solution and then heated until the powder was completely dissolved. The agarose solution was transferred into a cuvette and incubated at room temperature for more than 30 min, causing the phase transition to the gel state.

The absorption spectra of the gel were measured using a V-630 spectrophotometer (JASCO: Tokyo, Japan) at 20 °C. The phase transition of the gel was measured by monitoring the absorption at 750 nm using a UV-1800 spectrophotometer at heating and cooling rates of 0.5 °C min<sup>-1</sup>.

### 2.3. Measurement of the Stability of Oligonucleotide Structures in Agarose Gels

The fluorescence of DNA oligonucleotides in an agarose gel was measured in a 3-mm cuvette using an FP-8200 spectrofluorometer (JASCO). The agarose powder added to the buffer solution containing fluorescent dye-labeled oligonucleotides at a strand concentration of 0.5 µM (for intramolecular structures) or 1 µM (for intermolecular structures) was heated until dissolved, followed by incubation at room temperature for more than 30 min. Before the measurement of DNA melting, the oligonucleotides in the gel were heated at 60 °C for 10 min, which was lower than the gel-to-sol transition temperature, and then cooled to 0 °C at a rate of -0.5 °C min<sup>-1</sup>. After incubation at 0 °C for 10 min, melting and annealing curves of DNA structures were obtained by monitoring with an excitation wavelength of 491 nm and an emission wavelength of 518 nm. The melting curve was measured at a heating rate of 0.5 °C min<sup>-1</sup>, whereas the measurement at a heating rate of 0.2 °C min<sup>-1</sup> produced the same curve. The annealing curve was measured at a cooling rate of -0.5 °C min<sup>-1</sup>. The melting temperature,  $T_m$ , at which half of a DNA structure was denatured, and the annealing temperature,  $T_a$ , at which half of the structure was formed, were determined by nonlinear fitting of the melting and annealing curves, respectively [40], which were reproducible with errors of no more than 0.5 °C. The temperatures of the gel during the stability measurement of DNA structures were monitored using an SK-1250MCIII $\alpha$  thermocouple (Sato: Tokyo, Japan), which exhibited a difference of no more than 0.4 °C when tested with aqueous solutions.

### 2.4. Preparation of Polyacrylamide Gels and Measurement of the Stability of Oligonucleotide Structures in the Gels

Polyacrylamide gels were prepared by polymerizing acrylamide and  $N,N'$ -methylenebisacrylamide at a ratio of 19 to 1 in a 1 mL buffer solution at 50 °C, initiated by adding 0.05% ammonium persulfate and 0.05%  $N,N,N',N'$ -tetramethylethylenediamine (Wako Chemicals). Oligonucleotides were added either before or after the polymerization. In the former case, the gel was prepared by polymerization in the presence of oligonucleotides at 0.5 µM in a 10-mm cuvette. In the latter case, the gel was prepared by polymerization in the absence of oligonucleotides in a 10-mm cuvette. Then, the gel was washed by soaking it in 40 mL of distilled water and gently shaking it for 2 days at room temperature. The washed gel was dried in a vacuum using a vacuum pump DIVAC 0.6 L (Oerlikon: Zürich, Switzerland), and the dried gel was soaked in a 1 mL buffer solution

containing 0.5  $\mu\text{M}$  oligonucleotide at 4  $^{\circ}\text{C}$  to obtain a rehydrated gel. The weight of the gel during drying (the number of data samples  $n = 8$ ) and swelling ( $n = 3$ ) was measured using an AB204-s/FACT analytical balance (Mettler Toledo: Zürich, Switzerland), which was reproducible with errors of no more than 0.03 g (within the symbol sizes in the Figures given below). To prepare gels containing PEG, the dried gel was rehydrated with a 1 mL oligonucleotide solution containing 20% PEG with an average molecular weight of 200. Fluorescence images of fluorescent dye-labeled oligonucleotides in the gel, exhibiting weak emission of FAM even though a quencher is attached, were obtained using an FLA-7000 fluorescence scanner (Fujifilm: Tokyo, Japan).

Low-water-content polyacrylamide gels were prepared by treating the gel with a high-osmotic pressure solution of 20% PEG with an average molecular weight of  $2 \times 10^4$ . Rehydrated polyacrylamide gels were prepared under the condition, producing experimentally acceptable gels that contain oligonucleotides at 0.5  $\mu\text{M}$  (vacuum drying for 12 h followed by rehydration for 48 h, described in Section 3). The osmolyte solution containing oligonucleotides at 0.5  $\mu\text{M}$  was used for the transfer of water from the gel to the osmolyte solution due to the osmotic pressure difference across the surface. The 1 mL osmolyte solution was placed on the surface of the rehydrated gel in a 10-mm cuvette at room temperature, leading to a time-dependent reduction in the gel weight. The weight of the gel during the osmotic dehydration was calculated using the weight of the remaining solution after the gel was removed. The gel was incubated at room temperature for 24 h and then heated at 90  $^{\circ}\text{C}$  for 10 min and then cooled to 10  $^{\circ}\text{C}$  at a rate of  $-0.5 \text{ }^{\circ}\text{C min}^{-1}$ . After incubation at 10  $^{\circ}\text{C}$  for 10 min, melting and annealing curves of DNA structures were measured as described above. The temperatures of the gel during the stability measurement of DNA structures were monitored using a thermocouple, which exhibited a difference of no more than 0.2  $^{\circ}\text{C}$  when tested with aqueous solutions.

### 3. Results

#### 3.1. Stability Analysis of DNA Structures in Agarose Gels

The porous matrix of agarose gels formed by hydrogen bonds is disrupted at high temperatures. The agarose used in this study exhibited a reversible thermal phase transition: the heating and cooling curves exhibited hysteresis loops with the gel-to-sol transition ( $T_{\text{gel-to-sol}}$ ) temperature ranges of 60–85  $^{\circ}\text{C}$  and the sol-to-gel transition temperature ( $T_{\text{sol-to-gel}}$ ) ranges of 20–40  $^{\circ}\text{C}$ , depending on the gel concentration (Figure 1A). Based on the phase transition temperatures, several oligonucleotides that formed a defined secondary structure were designed. Because the gel exhibits strong absorption in the UV region, the measurement of changes in the UV absorbance of oligonucleotides, which is a convenient method for measuring the thermal stability of DNA structures, was inapplicable. As a result, we measured changes in the fluorescence intensity during thermal melting and annealing of DNA structures bearing FAM as a fluorophore and Dabcyl as a quencher: the formation of base-pair structures decreases the fluorescence intensity of FAM due to quenching by Dabcyl at a short distance (Figure 1B). We verified that the agarose gel exhibited low absorption at the excitation and emission wavelengths of FAM.

Figure 1C shows the fluorescence melting and annealing curves of a DNA duplex 5'-CTGGAT-3'/5'-ATCCAG-3' (6-mer DS) in the 5% agarose gel. DNA melting by heating occurred below the  $T_{\text{gel-to-sol}}$  and annealing by cooling occurred below the  $T_{\text{sol-to-gel}}$ , where no hysteresis was observed during the heating and cooling cycles. The melting temperature ( $T_m$ ) and annealing temperature ( $T_a$ ) of the DNA duplex in 0.5–5% agarose gels were approximately the same as those in the solution (Figure 1D). Other DNA sequences of different lengths and secondary structures were also analyzed: a 9-mer duplex 5'-CTTGCGTTG-3'/5'-CAACGCAAG-3' (9-mer DS); a 40-mer duplex 5'-ACTCACTATA<sub>21</sub>AGAAGAGATG-3'/5'-CATCTCTTCTA<sub>21</sub>ATAGTGAGT-3' (40-mer DS, forming an A<sub>21</sub>/A<sub>21</sub> internal loop); a 10-mer intramolecular hairpin 5'-ATCATGCGAT-3' (10-mer HP, forming an ATGC hairpin loop). The  $T_m$  values of these DNA structures in the 5% gel were lower than the  $T_{\text{gel-to-sol}}$ , whereas their  $T_a$  values were higher than the  $T_{\text{sol-to-gel}}$ , resulting in DNA melting in the

agarose in the gel state but annealing in the agarose in the sol state. Nonetheless, the  $T_m$  and  $T_a$  values of these structures were the same as those obtained in the solution (Figure 1E). These results show that the DNA secondary structures and equilibria for the structure formations are unaffected by the agarose both in the gel and sol states.

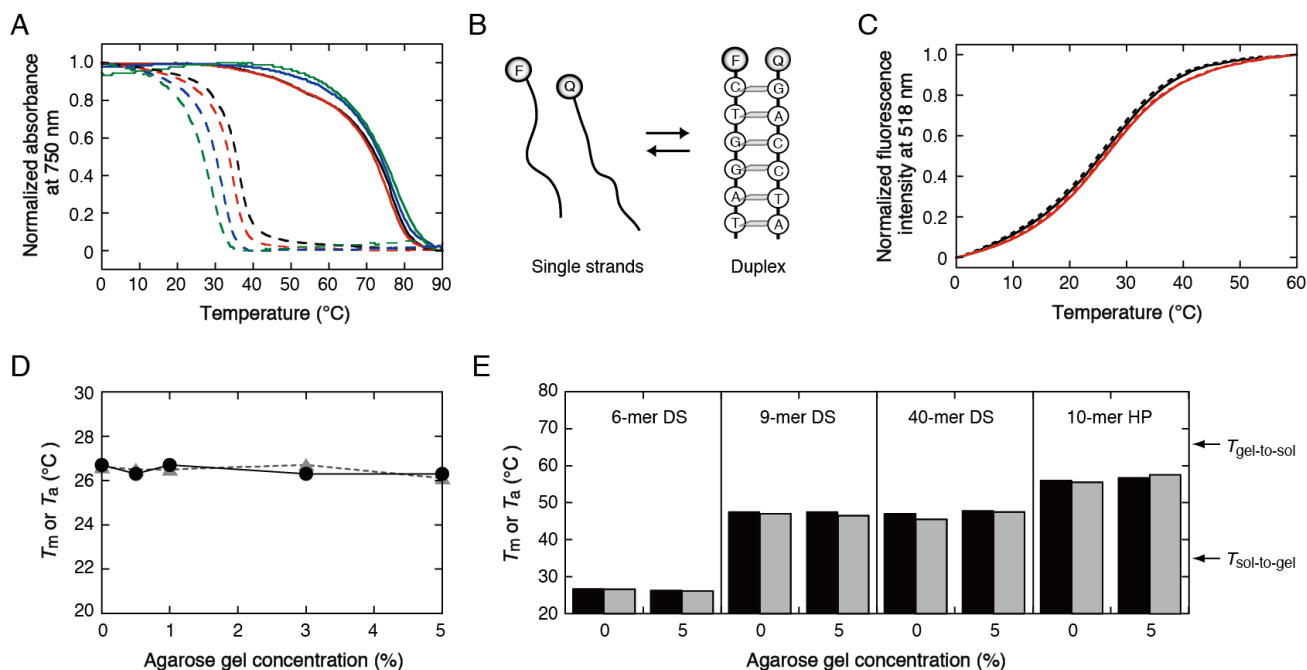


**Figure 1.** (A) Heating and cooling curves (solid and dotted lines, respectively) of agarose gels at 5% (black), 3% (red), 1% (blue), or 0.5% (green). (B) Equilibrium for the duplex formation of 6-mer DS by complementary single strands bearing a fluorophore, F, or a quencher, Q. (C) Melting and annealing curves (solid and dotted lines, respectively) of 6-mer DS in the 5% agarose gel (red) and the solution (black). (D) The  $T_m$  (black circles) and  $T_a$  (gray triangles) values of 6-mer DS in agarose gels at various concentrations. The values at 0% represent the temperatures obtained in the solution. (E) The  $T_m$  (black bars) and  $T_a$  (gray bars) values of DNA structures in the solution (represented as 0%) and the agarose gel at 5%.

PEG is a conventional reagent for investigating the effects of the molecular environment on nucleic acids [8]. The stability of oligonucleotide duplexes decreases in solutions containing low-molecular-weight PEG [41,42]. Here, we investigated the effect of PEG with an average molecular weight of 200 on 6-mer DS in the agarose gel. The gel containing PEG at 20% was transparent, and the degree of the PEG-induced  $T_m$  decrease in the gel was similar to the decrease in the solution (8.2 °C and 7.8 °C, respectively). It is likely that the internal environment of the agarose gel pore does not alter the effect of PEG on DNA base pairing.

### 3.2. Stability Analysis of DNA Structures in Polyacrylamide Gels

Acrylamide and bisacrylamide are crosslinked to create polyacrylamide gels, which are stable at high temperatures. When a 10% gel was prepared by polymerization in the presence of 10-mer HP (Figure 2A), the DNA melting curve exhibited steeply sloping low- and high-temperature baselines (a gray line in Figure 2B). Moreover, the DNA melting seemed to occur at a lower temperature than the melting in the solution (a black line in Figure 2B). An experiment using a solution containing unpolymerized acrylamide and bisacrylamide but lacking polymerization initiators also produced a melting curve exhibiting a  $T_m$  lower than that in the solution (a blue line in Figure 2B). Accordingly, the  $T_m$  decrease in the gel is probably caused by interactions of unpaired DNA bases with carbonyl groups of unpolymerized acrylamide, such as formamide and urea acting as nucleic

acid denaturants [43,44]. The unpolymerized monomers and polymerization initiators can be removed by immersing a polymerized gel in water as a washing solution. This method was successful for polynucleotides and relatively long oligonucleotides; however, it caused the leakage of short oligonucleotides embedded in the gel to the washing solution.

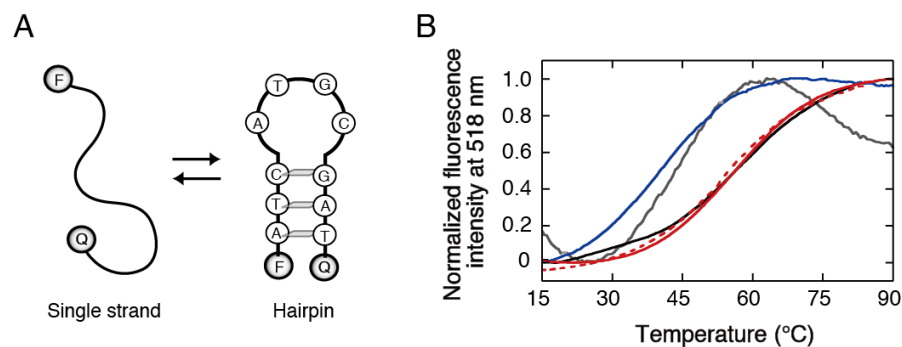


**Figure 2.** (A) Equilibrium for the hairpin formation of 10-mer HP by a single strand bearing a fluorophore, F, and a quencher, Q. (B) Melting curves of 10-mer HP in the solution (black), the solution containing unpolymerized acrylamide and bisacrylamide at 10% (blue), and unwashed and washed polyacrylamide gels at 10% (gray and red, respectively). The dotted line represents the annealing curve in the washed gel.

The embedding of oligonucleotides after washing a preformed gel was tested. In this preparation method, acrylamide and bisacrylamide were polymerized in the absence of oligonucleotides, and the polymerized gel was immersed in and washed with an excess amount of distilled water for 2 days. The washed gel was dried in a vacuum, yielding a shrunken gel. Quick vacuum drying (taking within a few hours) did not produce a transparent gel after rehydration of the dried gel with the buffer solution. In contrast, experimentally acceptable gels were obtained by applying a slow vacuum condition (taking approximately 10 h for drying): the weight of a 10% gel prepared with a 1 mL solution gradually decreased with the drying time (Figure 3A), and the weight after 10 h drying (approximately 0.1 g) corresponded to the weight of the matrix of the gel at 10%. The dried gel was subsequently transferred to a 1 mL buffer solution containing oligonucleotides. The weight of the gel increased as the swelling time increased and grew to over 0.9 g after 30 h (Figure 3B). The rehydrated gel had low absorption at the excitation and emission wavelengths of FAM, and the absorption did not change over the DNA melting temperature range. When an unwashed gel was dried in a vacuum, the gel became white because of undissolved salt deposits, and the salts were not dissolved by immersing the gel in water. Based on these test results, the polyacrylamide gels used for DNA melting were prepared by washing a gel with water, followed by slow vacuum drying for 12 h and rehydration with the buffer solution containing oligonucleotides for 48 h. Fluorescence imaging of fluorescent dye-labeled 10-mer HP in the gel and its crushed pieces showed an apparently uniform distribution in the gel prepared as above (Figure 3C).

Because it was difficult to evaluate the oligonucleotide concentration embedded in polyacrylamide gels, intramolecularly folded structures with the  $T_m$  independent of the oligonucleotide concentration were analyzed. The melting and annealing curves of 10-mer HP in the 10% gel (red lines in Figure 2B) were approximately the same as those in the solution. We also examined the human telomere DNA sequence 5'-(G<sub>3</sub>T<sub>2</sub>A)<sub>3</sub>G<sub>3</sub>-3' bearing FAM and TAMRA (21-mer GQ), which forms an intramolecular structure consisting of tetrads of hydrogen-bonded guanine bases known as a G-quadruplex (GQ) (Figure 4A) [45]. The formation of the G-quadruplex structure was confirmed by measuring circular dichroism spectra. The G-quadruplex exhibited no hysteresis between the melting and annealing curves in the gel (Figure 4B), and the stability was unchanged at different gel concentrations, as observed for 10-mer HP (Figure 4C).

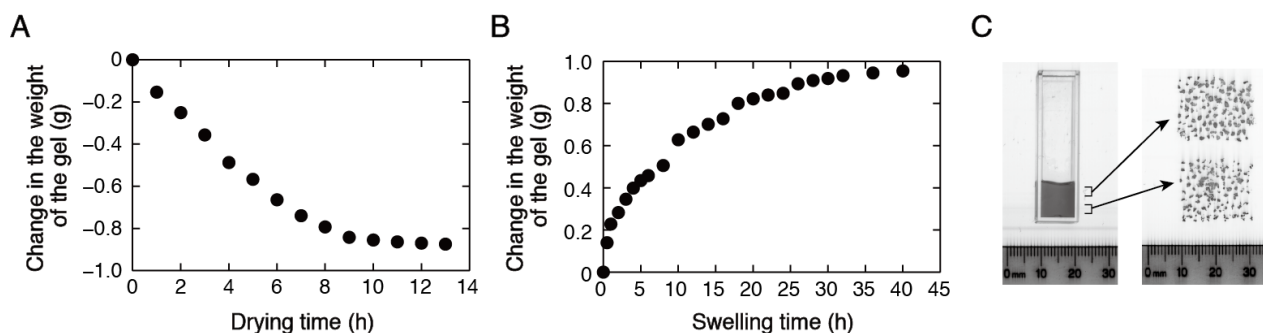


**Figure 3.** (A) The drying time-dependent change in the weight of the 10% polyacrylamide gel prepared with a 1 mL solution. (B) The swelling time-dependent change in the weight of the dried polyacrylamide gel. (C) Fluorescence images of fluorescent dye-labeled 10-mer HP in the 10% polyacrylamide gel prepared in a 10-mm cuvette (left) and crushed pieces of the upper and lower parts of the gel in the cuvette (right).

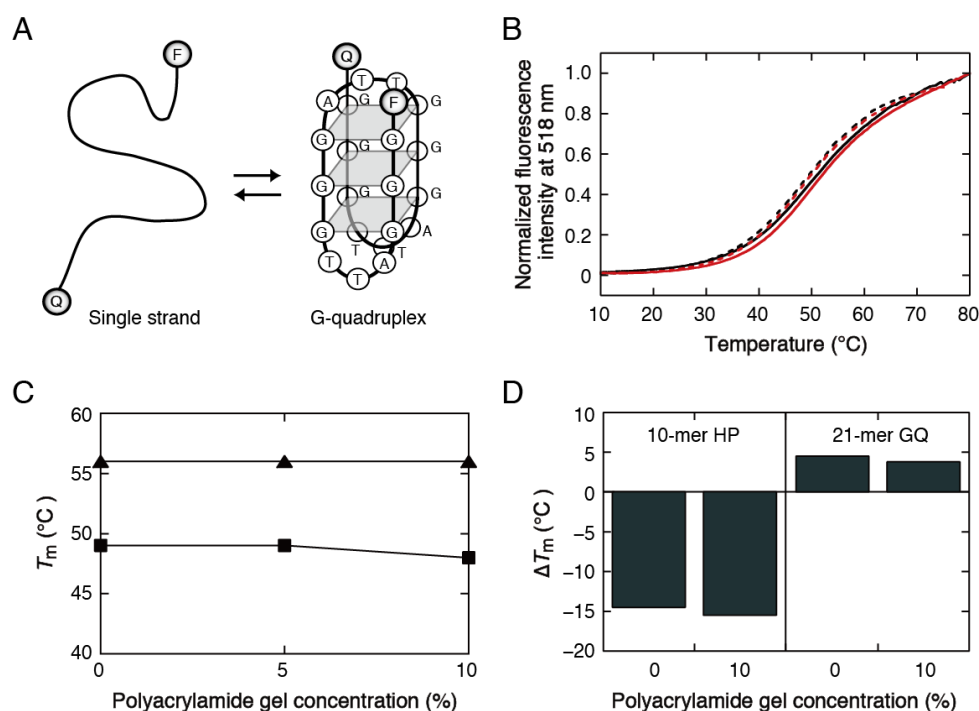


**Figure 4.** (A) Equilibrium for the G-quadruplex formation of 21-mer GQ by a single strand bearing a fluorophore, F, and a quencher, Q. (B) Melting and annealing curves (solid and dotted lines, respectively) of 21-mer GQ in the 10% polyacrylamide gel (red) and the solution (black). (C) The  $T_m$  values of 10-mer HP (triangles) and 21-mer GQ (squares) in the solution (represented as 0%) and the polyacrylamide gels at various concentrations. (D) Changes in the  $T_m$  values of 10-mer HP and 21-mer GQ by the addition of PEG with an average molecular weight of 200 to the solution (represented as 0%) and the polyacrylamide gel at 10%.

We also investigated the effect of PEG with an average molecular weight of 200 on the stability of the DNA structures in the polyacrylamide gel. To prepare polyacrylamide gels containing PEG, the dried gel was rehydrated with a PEG-containing solution, forming a transparent gel. The presence of PEG at 20% in the gel decreased the  $T_m$  of 10-mer HP from 56.0 °C to 41.5 °C but increased the  $T_m$  of 21-mer GQ from 48.0 °C to 51.8 °C. The degrees of their  $T_m$  changes by the addition of PEG were similar to those obtained in the solution (Figure 4D). It is likely that the internal environment of the polyacrylamide gel pore does not alter the effect of PEG on the DNA interactions.

### 3.3. Stability Analysis of DNA Structures in Low-Water-Content Gels

The experimental system using a polyacrylamide gel was also used to assess the stability of DNA structures under the conditions of a reduced number of water molecules. The gel can be dehydrated by treating it with a high-osmotic pressure solution. We used high-molecular-weight PEG with an average molecular weight of  $2 \times 10^4$  as an osmolyte. This polymer is sufficiently large compared with the pore size of the polyacrylamide gel and thus cannot penetrate the gel matrix. In addition, the polymer does not affect the stability of oligonucleotide structures in the buffer solution [46]. The osmotic pressure difference across the surface, causing the transfer of water from the gel to the osmolyte solution, led to a time-dependent reduction in the gel weight (Figure 5A). The gel weight was gradually reduced over several hours, producing a slightly shrunken but transparent gel. Analysis of intramolecular DNA melting using the gels obtained at different time points, and consequently at different degrees of dehydration, showed that the  $T_m$  of 10-mer HP decreased with the time of osmotic dehydration in a similar manner to the changes in the gel weight (Figure 5B). Conversely, the  $T_m$  of 21-mer GQ increased with the time of osmotic dehydration; however, the  $T_m$  changed in a similar manner to the changes in the gel weight.

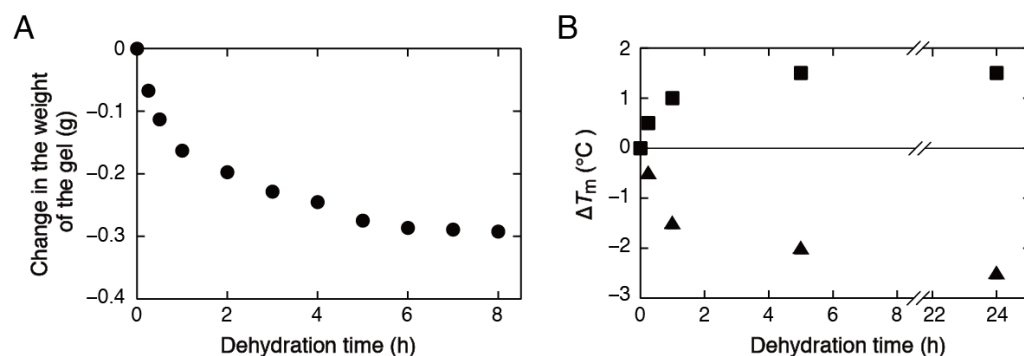


**Figure 5.** (A) Changes in the weight of a 10% polyacrylamide gel by dehydration using a high-osmotic pressure solution. (B) Changes in the  $T_m$  values of 10-mer HP (triangles) and 21-mer GQ (squares) in the gels prepared by osmotic dehydration at different time points, compared with the  $T_m$  in the solution.

## 4. Discussion

We developed methods for preparing agarose and polyacrylamide gels used to evaluate the stability of oligonucleotide structures embedded in these gels. The hydrogels used in this study have different filament structures and pore sizes. The agarose gel forms a three-dimensional matrix of hydrogen-bonded bundles of linear polysaccharide chains. The pore size is heterogeneous; however, it ranges roughly from a few tens of nanometers to a few micrometers: the size of a 0.5% gel is approximately 200 nm and that of a 5% gel is approximately 55 nm even though the size is also influenced by the preparation conditions such as temperature and the ionic strength [47–49]. Our study demonstrated that DNA melting in agarose gels at high concentrations could be measured using oligonucleotides bearing fluorescent probes. On the other hand, the pore size of polyacrylamide gels formed by the polymerization of acrylamide and bisacrylamide at high concentrations is a few tens of nanometers or smaller than 10 nm [50,51], which is comparable to the distance between cytoskeleton fibers in cells. Our study demonstrated that polyacrylamide gels are required to be washed before being used to measure DNA melting. We successfully prepared polyacrylamide gels embedding oligonucleotides by rehydrating a washed dry gel with the solution containing oligonucleotides.

The oligonucleotides in the gel pores are spatially confined and have reduced conformational space and translational motion. The thermal melting profile of DNA structures is changed if the confinement affects the stability of DNA base pairing in terms of changes in

the entropy and enthalpy of DNA interactions. However, the oligonucleotide structures exhibited reversible thermal transitions in both gels, and the  $T_m$  and  $T_a$  values and shape of the melting curves were the same as those obtained in the solution. The findings show that the oligonucleotides used in this study, with a diameter of gyration roughly ranging from 2 to 6 nm [52,53], which are comparable to or smaller than the pore size of the gels, are not strongly constrained in the gels. In contrast, the previous study using DNA polynucleotides showed an increase in the stability of a long duplex embedded in polyacrylamide gels [39], consistent with reported computer simulation and experimental studies [26–31,33,35,37,38]. It is possible that the short oligonucleotides, promising for applications in the fields of biotechnology and nanotechnology, are too short to experience the spatial confinement in the gels. It is also conceivable that the oligonucleotides are preferentially located in less confined spaces in the gel matrix.

The environment in the gel matrix has distinctive solvent properties and may produce binding interactions of DNA with gel filaments. Our results reveal that the influence of changes in the solvent properties of water, such as viscosity, molecular activity, and dielectric constant, was insignificant. Besides, oligonucleotide interactions are not strongly perturbed by the gel matrix. The findings are inconsistent with the reports on proteins and oligopeptides that showed confinement-induced stabilization and significant effects on the surface of gel filaments [22–25,54,55], possibly because of differences in the chemical structure and flexibility between amino acid and nucleotide chains. The gels used in this study have many polar groups that can act as hydrogen bond donors and acceptors: hydroxyl groups in the agarose gel, and carbamoyl and secondary amide groups in the polyacrylamide gel. A simple calculation indicates that the average densities of the polar groups in space of the 5% agarose gel and 10% polyacrylamide gel were similar to each other (approximately 1 functional group per square nanometer), and also to the densities of hydroxyl groups of PEG in its 20% solution used in Figure 4D and carbamoyl and secondary amide groups of acrylamide and bisacrylamide in their mixed 10% solution used in Figure 2B. Nonetheless, unlike the PEG- and acrylamide-dissolved solutions, the gel filaments did not affect the  $T_m$  of the oligonucleotide structures. These observations suggest that the polar groups attached to gel filaments, such as hydroxyl, carbamoyl, and secondary amide groups, are unsuitable for interacting with oligonucleotides. It is likely that the oligonucleotides are excluded from the surface of gel filaments and may be preferentially located in a water-rich environment in the gel matrix. This possibility was supported by the results that the  $T_m$  changes of 10-mer HP and 21-mer GQ by the addition of PEG were similar in the gel and the solution, indicating a superior influence of the solvent components in the gels over the gel matrix. The finding that the self-assembly and hybridization of short oligonucleotides are unaffected by the gel matrix provides a basis for quantitative analyses of oligonucleotide structures and interactions using in-gel assays such as gel shift and temperature gradient gel electrophoresis assays.

DNA is highly hydrated, and the degree of hydration differs between different DNA structures. Because the addition of low-molecular-weight PEG reduces the water activity of a solution, its opposing effects on 10-mer HP and 21-mer GQ can be accounted for by the differences in water contributions to structure formations: the hairpin formation is the net hydration reaction, and the G-quadruplex formation is the net dehydration reaction [42,56]. The contribution of PEG binding to nucleotide bases can also be considered: hydrophobic interactions with single-stranded DNA bases disrupt or weaken base pairing of the hairpin structure, whereas interactions with the plane of four guanine bases stabilize the G-quadruplex structure [41,57,58]. The study using low-water-content gels enabled a direct test of the effects of reduced water content on DNA structure formations. We observed decreases in the  $T_m$  of 10-mer HP and increases in the  $T_m$  of 21-mer GQ by reducing the number of water molecules in the gel, indicating that the availability of water molecules affects the stability of these DNA structures. However, the degrees of  $T_m$  changes in low-water-content gels were smaller than those in PEG-containing solutions, particularly in the case of 10-mer HP. It is possible that the contribution of PEG binding

to single-stranded DNA bases is significant. It can also be speculated that the internal environment of the gel pores has a buffering effect on the reduction in the number of water molecules. Further studies would be helpful for understanding the effects of water content on the stability of DNA structures.

## 5. Conclusions

We demonstrated the preparation of hydrogels for evaluating the stability of DNA duplex, hairpin, and G-quadruplex structures, which is promising for application in the fields of biotechnology and nanotechnology in confined spaces. The preparation of oligonucleotides embedded in hydrogen-bonded filament networks of the agarose gel was simple, whereas the preparation of oligonucleotides embedded in crosslinked filament networks of the polyacrylamide gel was required to rehydrate a washed dry gel with a buffer solution containing oligonucleotides. The thermodynamic studies revealed that the oligonucleotides formed self-assembled structures and hybridization complexes in the gels with similar stabilities to those in solutions. The results indicate that the oligonucleotide structures are unperturbed by confinement in the gel pores and chemical groups of the gel filaments. The superior influence of the solvent components in the gels over the gel matrix implies a preferential location of oligonucleotides in a water-rich environment in the gel matrix. We also demonstrated the application of the gel to the assessment of the stability of DNA structures under the conditions of a reduced number of water molecules. These findings will benefit the design of DNA sequences used for in-gel assays and the investigation of the stability of DNA structures under low-water-content conditions. The preparation methods developed in this study could be applicable to other types of hydrogels with different filament networks.

**Author Contributions:** Conceptualization, S.-i.N. and D.Y.; Data Acquisition and Analysis, S.-i.N., D.Y. and M.Y.; Writing and Funding Acquisition, S.-i.N. All authors have read and agreed to the published version of the manuscript.

**Funding:** This research was funded in part by Grants-in-Aid for Scientific Research, Japan Society for the Promotion of Science (JSPS KAKENHI, grant number 24550200).

**Institutional Review Board Statement:** Not applicable.

**Informed Consent Statement:** Not applicable.

**Data Availability Statement:** The data presented in this study is available in the article.

**Conflicts of Interest:** The authors declare that they have no conflicts of interest.

## References

1. Turner, D.H. Conformational Changes. In *Nucleic Acids: Structures, Properties and Functions*; Bloomfield, V.A., Crothers, D.M., Tinoco, J.L., Eds.; University Science Books Press: Sausalito, CA, USA, 2000; pp. 259–334.
2. Zhou, H.X.; Rivas, G.; Minton, A.P. Macromolecular crowding and confinement: Biochemical, biophysical, and potential physiological consequences. *Annu. Rev. Biophys.* **2008**, *37*, 375–397. [[CrossRef](#)] [[PubMed](#)]
3. Mika, J.T.; Poolman, B. Macromolecule diffusion and confinement in prokaryotic cells. *Curr. Opin. Biotechnol.* **2011**, *22*, 117–126. [[CrossRef](#)] [[PubMed](#)]
4. Castronovo, M.; Stopar, A.; Coral, L.; Redhu, S.K.; Vidonis, M.; Kumar, V.; Ben, F.D.; Grassi, M.; Nicholson, A.W. Effects of nanoscale confinement on the functionality of nucleic acids: Implications for nanomedicine. *Curr. Med. Chem.* **2013**, *20*, 3539–3557. [[CrossRef](#)] [[PubMed](#)]
5. Elder, R.M.; Pfaendtner, J.; Jayaraman, A. Effect of hydrophobic and hydrophilic surfaces on the stability of double-stranded DNA. *Biomacromolecules* **2015**, *16*, 1862–1869. [[CrossRef](#)]
6. Gao, M.; Gnutt, D.; Orban, A.; Appel, B.; Righetti, F.; Winter, R.; Narberhaus, F.; Muller, S.; Ebbinghaus, S. RNA hairpin folding in the crowded cell. *Angew. Chem. Int. Ed. Engl.* **2016**, *55*, 3224–3228. [[CrossRef](#)] [[PubMed](#)]
7. Ganser, L.R.; Kelly, M.L.; Herschlag, D.; Al-Hashimi, H.M. The roles of structural dynamics in the cellular functions of RNAs. *Nat. Rev. Mol. Cell. Biol.* **2019**, *20*, 474–489. [[CrossRef](#)] [[PubMed](#)]
8. Nakano, S.; Miyoshi, D.; Sugimoto, N. Effects of molecular crowding on the structures, interactions, and functions of nucleic acids. *Chem. Rev.* **2014**, *114*, 2733–2758. [[CrossRef](#)]

9. Riback, J.A.; Katanski, C.D.; Kear-Scott, J.L.; Pilipenko, E.V.; Rojek, A.E.; Sosnick, T.R.; Drummond, D.A. Stress-triggered phase separation Is an adaptive, evolutionarily tuned response. *Cell* **2017**, *168*, 1028–1040.e19. [[CrossRef](#)] [[PubMed](#)]
10. Jun, S.; Mulder, B. Entropy-driven spatial organization of highly confined polymers: Lessons for the bacterial chromosome. *Proc. Natl. Acad. Sci. USA* **2006**, *103*, 12388–12393. [[CrossRef](#)]
11. Buenemann, M.; Lenz, P. A geometrical model for DNA organization in bacteria. *PLoS ONE* **2010**, *5*, e13806. [[CrossRef](#)]
12. Yanagisawa, M.; Sakaue, T.; Yoshikawa, K. Characteristic behavior of crowding macromolecules confined in cell-sized droplets. *Int. Rev. Cell Mol. Biol.* **2014**, *307*, 175–204.
13. Gursoy, G.; Xu, Y.; Liang, J. Spatial organization of the budding yeast genome in the cell nucleus and identification of specific chromatin interactions from multi-chromosome constrained chromatin model. *PLoS Comput. Biol.* **2017**, *13*, e1005658. [[CrossRef](#)] [[PubMed](#)]
14. Lin, J.C.; Hsu, C.Y.; Chen, J.Y.; Fang, Z.S.; Chen, H.W.; Yao, B.Y.; Shiao, G.H.M.; Tsai, J.S.; Gu, M.; Jung, M.; et al. Facile transformation of murine and human primary dendritic cells into robust and modular artificial antigen-presenting systems by intracellular hydrogelation. *Adv. Mater.* **2021**, *33*, e2101190. [[CrossRef](#)] [[PubMed](#)]
15. Macdougall, L.J.; Hoffman, T.E.; Kirkpatrick, B.E.; Fairbanks, B.D.; Bowman, C.N.; Spencer, S.L.; Anseth, K.S. Intracellular crowding by bio-orthogonal hydrogel formation induces reversible molecular stasis. *Adv. Mater.* **2022**, *34*, e2202882. [[CrossRef](#)] [[PubMed](#)]
16. Reisner, W.; Pedersen, J.N.; Austin, R.H. DNA confinement in nanochannels: Physics and biological applications. *Rep. Prog. Phys.* **2012**, *75*, 106601. [[CrossRef](#)]
17. Hoffman, A.S. Hydrogels for biomedical applications. *Adv. Drug Deliv. Rev.* **2002**, *54*, 3–12. [[CrossRef](#)]
18. Morya, V.; Walia, S.; Mandal, B.B.; Ghoroi, C.; Bhatia, D. Functional DNA based hydrogels: Development, properties and biological applications. *ACS Biomater. Sci. Eng.* **2020**, *6*, 6021–6035. [[CrossRef](#)]
19. Zhu, Y.; Granick, S. Viscosity of interfacial water. *Phys. Rev. Lett.* **2001**, *87*, 096104. [[CrossRef](#)]
20. Raviv, U.; Laurat, P.; Klein, J. Fluidity of water confined to subnanometre films. *Nature* **2001**, *413*, 51–54. [[CrossRef](#)]
21. Perez-Hernandez, N.; Luong, T.Q.; Perez, C.; Martin, J.D.; Havenith, M. Pore size dependent dynamics of confined water probed by FIR spectroscopy. *Phys. Chem. Chem. Phys.* **2010**, *12*, 6928–6932. [[CrossRef](#)]
22. Zhou, H.X.; Dill, K.A. Stabilization of proteins in confined spaces. *Biochemistry* **2001**, *40*, 11289–11293. [[CrossRef](#)] [[PubMed](#)]
23. Mittal, J.; Best, R.B. Thermodynamics and kinetics of protein folding under confinement. *Proc. Natl. Acad. Sci. USA* **2008**, *105*, 20233–20238. [[CrossRef](#)] [[PubMed](#)]
24. Eggers, D.K.; Valentine, J.S. Crowding and hydration effects on protein conformation: A study with sol-gel encapsulated proteins. *J. Mol. Biol.* **2001**, *314*, 911–922. [[PubMed](#)]
25. Cheung, M.S.; Thirumalai, D. Nanopore-protein interactions dramatically alter stability and yield of the native state in restricted spaces. *J. Mol. Biol.* **2006**, *357*, 632–643. [[CrossRef](#)] [[PubMed](#)]
26. Tan, Z.J.; Chen, S.J. Ion-mediated RNA structural collapse: Effect of spatial confinement. *Biophys. J.* **2012**, *103*, 827–836. [[CrossRef](#)]
27. Feng, C.; Tan, Y.L.; Cheng, Y.X.; Shi, Y.Z.; Tan, Z.J. Salt-dependent RNA pseudoknot stability: Effect of spatial confinement. *Front. Mol. Biosci.* **2021**, *8*, 666369. [[CrossRef](#)] [[PubMed](#)]
28. Li, H.; Wang, Z.; Li, N.; He, X.; Liang, H. Denaturation and renaturation behaviors of short DNA in a confined space. *J. Chem. Phys.* **2014**, *141*, 044911. [[CrossRef](#)]
29. Reiter-Schad, M.; Werner, E.; Tegenfeldt, J.O.; Mehlig, B.; Ambjornsson, T. How nanochannel confinement affects the DNA melting transition within the Poland-Scheraga model. *J. Chem. Phys.* **2015**, *143*, 115101. [[CrossRef](#)]
30. Maity, A.; Singh, N. Melting of DNA in confined geometries. *Eur. Biophys. J.* **2020**, *49*, 561–569. [[CrossRef](#)]
31. Pal, S.; Paul, S. Theoretical investigation of conformational deviation of the human parallel telomeric G-quadruplex DNA in the presence of different salt concentrations and temperatures under confinement. *Phys. Chem. Chem. Phys.* **2021**, *23*, 14372–14382. [[CrossRef](#)]
32. Chen, I.A.; Salehi-Ashtiani, K.; Szostak, J.W. RNA catalysis in model protocell vesicles. *J. Am. Chem. Soc.* **2005**, *127*, 13213–13219. [[CrossRef](#)] [[PubMed](#)]
33. Pramanik, S.; Nagatoishi, S.; Sugimoto, N. DNA tetraplex structure formation from human telomeric repeat motif (TTAGGG)<sub>n</sub>(CCCTAA)<sub>n</sub> in nanocavity water pools of reverse micelles. *Chem. Commun.* **2012**, *48*, 4815–4817. [[CrossRef](#)] [[PubMed](#)]
34. Strulson, C.A.; Molden, R.C.; Keating, C.D.; Bevilacqua, P.C. RNA catalysis through compartmentalization. *Nat. Chem.* **2012**, *4*, 941–946. [[CrossRef](#)] [[PubMed](#)]
35. Shrestha, P.; Jonchhe, S.; Emura, T.; Hidaka, K.; Endo, M.; Sugiyama, H.; Mao, H. Confined space facilitates G-quadruplex formation. *Nat. Nanotechnol.* **2017**, *12*, 582–588. [[CrossRef](#)]
36. Jonchhe, S.; Pandey, S.; Emura, T.; Hidaka, K.; Hossain, M.A.; Shrestha, P.; Sugiyama, H.; Endo, M.; Mao, H. Decreased water activity in nanoconfinement contributes to the folding of G-quadruplex and i-motif structures. *Proc. Natl. Acad. Sci. USA* **2018**, *115*, 9539–9544. [[CrossRef](#)]
37. Downs, A.M.; McCallum, C.; Pennathur, S. Confinement effects on DNA hybridization in electrokinetic micro- and nanofluidic systems. *Electrophoresis* **2019**, *40*, 792–798. [[CrossRef](#)]
38. Jonchhe, S.; Pandey, S.; Karna, D.; Pokhrel, P.; Cui, Y.; Mishra, S.; Sugiyama, H.; Endo, M.; Mao, H. Duplex DNA is weakened in nanoconfinement. *J. Am. Chem. Soc.* **2020**, *142*, 10042–10049. [[CrossRef](#)]

39. Nakano, S.; Yamaguchi, D.; Sugimoto, N. Thermal stability and conformation of DNA and proteins under the confined condition in the matrix of hydrogels. *Mol. Biol. Rep.* **2018**, *45*, 403–411. [[CrossRef](#)]
40. Puglisi, J.D.; Tinoco, I., Jr. Absorbance melting curves of RNA. *Methods. Enzymol.* **1989**, *180*, 304–325.
41. Knowles, D.B.; LaCroix, A.S.; Deines, N.F.; Shkel, I.; Record, M.T., Jr. Separation of preferential interaction and excluded volume effects on DNA duplex and hairpin stability. *Proc. Natl. Acad. Sci. USA* **2011**, *108*, 12699–12704. [[CrossRef](#)]
42. Nakano, S.; Yamaguchi, D.; Tateishi-Karimata, H.; Miyoshi, D.; Sugimoto, N. Hydration changes upon DNA folding studied by osmotic stress experiments. *Biophys. J.* **2012**, *102*, 2808–2817. [[CrossRef](#)] [[PubMed](#)]
43. Blake, R.D.; Delcourt, S.G. Thermodynamic effects of formamide on DNA stability. *Nucleic Acids Res.* **1996**, *24*, 2095–2103. [[CrossRef](#)] [[PubMed](#)]
44. Nordstrom, L.J.; Clark, C.A.; Andersen, B.; Champlin, S.M.; Schweinfus, J.J. Effect of ethylene glycol, urea, and *N*-methylated glycines on DNA thermal stability: The role of DNA base pair composition and hydration. *Biochemistry* **2006**, *45*, 9604–9614. [[CrossRef](#)] [[PubMed](#)]
45. Williamson, J.R. G-quartet structures in telomeric DNA. *Annu. Rev. Biophys. Biomol. Struct.* **1994**, *23*, 703–730. [[CrossRef](#)] [[PubMed](#)]
46. Nakano, S.; Wu, L.; Oka, H.; Karimata, H.T.; Kirihata, T.; Sato, Y.; Fujii, S.; Sakai, H.; Kuwahara, M.; Sawai, H.; et al. Conformation and the sodium ion condensation on DNA and RNA structures in the presence of a neutral cosolute as a mimic of the intracellular media. *Mol. BioSyst.* **2008**, *4*, 579–588. [[CrossRef](#)] [[PubMed](#)]
47. Maaloum, M.; Pernodet, N.; Tinland, B. Agarose gel structure using atomic force microscopy: Gel concentration and ionic strength effects. *Electrophoresis* **1998**, *19*, 1606–1610. [[CrossRef](#)]
48. Xiong, J.Y.; Narayanan, J.; Liu, X.Y.; Chong, T.K.; Chen, S.B.; Chung, T.S. Topology evolution and gelation mechanism of agarose gel. *J. Phys. Chem. B* **2005**, *109*, 5638–5643. [[CrossRef](#)]
49. Zhou, J.; Zhou, M.; Caruso, R.A. Agarose template for the fabrication of macroporous metal oxide structures. *Langmuir* **2006**, *22*, 3332–3336. [[CrossRef](#)]
50. Haggerty, L.; Sugarman, J.H.; Prud'homme, R.K. Diffusion of polymers through polyacrylamide gels. *Polymer* **1988**, *29*, 1058–1063. [[CrossRef](#)]
51. Holmes, D.L.; Stellwagen, N.C. Estimation of polyacrylamide gel pore size from Ferguson plots of linear DNA fragments. II. Comparison of gels with different crosslinker concentrations, added agarose and added linear polyacrylamide. *Electrophoresis* **1991**, *12*, 612–619. [[CrossRef](#)]
52. Sim, A.Y.; Lipfert, J.; Herschlag, D.; Doniach, S. Salt dependence of the radius of gyration and flexibility of single-stranded DNA in solution probed by small-angle x-ray scattering. *Phys. Rev. E* **2012**, *86*, 021901. [[CrossRef](#)] [[PubMed](#)]
53. Plumridge, A.; Meisburger, S.P.; Pollack, L. Visualizing single-stranded nucleic acids in solution. *Nucleic Acids Res.* **2017**, *45*, e66. [[CrossRef](#)] [[PubMed](#)]
54. Rao, J.S.; Cruz, L. Effects of confinement on the structure and dynamics of an intrinsically disordered peptide: A molecular-dynamics study. *J. Phys. Chem. B* **2013**, *117*, 3707–3719. [[CrossRef](#)] [[PubMed](#)]
55. Rao, J.S.; Smith, M.D.; Cruz, L. The stability of a beta-hairpin is altered by surface-water interactions under confinement. *J. Phys. Chem. B* **2014**, *118*, 3517–3523. [[CrossRef](#)]
56. Miyoshi, D.; Karimata, H.; Sugimoto, N. Hydration regulates thermodynamics of G-quadruplex formation under molecular crowding conditions. *J. Am. Chem. Soc.* **2006**, *128*, 7957–7963. [[CrossRef](#)]
57. Buscaglia, R.; Miller, M.C.; Dean, W.L.; Gray, R.D.; Lane, A.N.; Trent, J.O.; Chaires, J.B. Polyethylene glycol binding alters human telomere G-quadruplex structure by conformational selection. *Nucleic Acids Res.* **2013**, *41*, 7934–7946. [[CrossRef](#)]
58. Nakano, M.; Tateishi-Karimata, H.; Tanaka, S.; Tama, F.; Miyashita, O.; Nakano, S.; Sugimoto, N. Local thermodynamics of the water molecules around single- and double-stranded DNA studied by grid inhomogeneous solvation theory. *Chem. Phys. Lett.* **2016**, *660*, 250–255. [[CrossRef](#)]